IEEE Access
Multidisciplinary ⋮ Rapid Review ⋮ Open Access Journal

Received February 13, 2022, accepted March 16, 2022, date of publication March 22, 2022, date of current version April 1, 2022.

Digital Object Identifier 10.1109/ACCESS.2022.3161467

An Effective Optimization Algorithm for Parameters Identification of Photovoltaic Models

BEHDAD ARANDIAN[1], MAHDIYEH ESLAMI[2], (Member, IEEE), SAIFULNIZAM ABD. KHALID[3], BASEEM KHAN[4], (Senior Member, IEEE), USMAN ULLAH SHEIKH[3], (Senior Member, IEEE), EHSAN AKBARI[5], AND ADIL HUSSEIN MOHAMMED[6]

[1] 1Department of Electrical Engineering, Dolatabad Branch, Islamic Azad University, Isfahan 8441811111, Iran
[2]Department of Electrical Engineering, Kerman Branch, Islamic Azad University, Kerman 7635168111, Iran
[3]School of Electrical Engineering, Faculty of Engineering, Universiti Teknologi Malaysia, Johor Bahru 81310, Malaysia
[4]Department of Electrical and Computer Engineering, Hawassa University, Hawassa 05, Ethiopia
[5]Faculty of Electrical and Computer Engineering Mazandaran University of Science and Technology, Babol 4851878195, Iran
[6]Department of Communication and Computer Engineering, Faculty of Engineering, Cihan University-Erbil, Kurdistan Region, Erbil 44001, Iraq

Corresponding authors: Mahdiyeh Eslami (mahdiyeh_eslami@yahoo.com) and Baseem Khan (baseem.khan04@gmail.com)

ABSTRACT Renewable energy is becoming more popular due to environmental concerns about the previous energy source. Accurate solar photovoltaic (PV) system model parameters substantially impact the efficiency of solar energy conversion to electricity. In this matter, swarm and evolutionary optimization algorithms have been widely utilized in dealing with practical problems due to their more straightforward concepts, efficacy, flexibility, and easy-to-implement procedural frameworks. However, the nonlinearity and complexity of the PV parameter identification caused swarm and evolutionary optimizers to exhibit Immaturity in the obtained solutions. In this study, an effective metaheuristic algorithm based on tunicate swarm optimization (TSA) is proposed for parameter identification of PV models. The proposed improved algorithm (ITSA) has two main phases at each iteration: searching all around the search space based on a randomly selected tunicate and improving the search using the position of the best tunicate. This modification improves the algorithm's exploration ability while also preventing premature convergence. The suggested algorithm's performance is confirmed using ten mathematical test functions and the outcomes are compared with TSA as well as some effective optimization algorithms. The proposed ITSA optimally identifies various parameters in the PV model, such as single diode (SDM), double diode (DDM), and PV modules. Based on the comprehensive comparisons, results indicate that the improved ITSA algorithm has higher convergence accuracy and better stability than the original TSA and other studied algorithms.

INDEX TERMS Tunicate swarm optimization, photovoltaic model, solar energy, parameter identification.

I. INTRODUCTION

Considering some critical challenges, such as but not limited to environmental pollution, energy crisis, fuel exhaustion, climate change, we will understand the significance of renewable energy sources in which they play an essential role in our daily life. As a clean and attainable renewable energy source, PV is categorized among the most potential cell-based energy source. One of the major causes of these catastrophes is environmental degradation caused by the burning of fossil fuels. Furthermore, fossil fuel reserves are finite and unrecoverable. Given the drawbacks of fossil fuels, discovering renewable energy sources is a pressing human concern.

Due to its lack of noise, low pollution, and widespread distribution, solar energy appears to be the most promising renewable energy source [1]. Severe environmental degradation, such as deforestation and air pollution [2], as well as rapid depletion of nonrenewable resources such as traditional fossil fuels [3], is jeopardizing the world's long-term development [4]. A long-term energy revolution and transformation are now required to deal with a wide range of environmental problems before they turn into more serious crises [5]. Meanwhile, to satisfy the rising energy demand [6], the research and use of renewable energy technologies [7], such as solar [8] and wind [9], is critical. Solar energy is

The associate editor coordinating the review of this manuscript and approving it for publication was Sotirios Goudos.

one of the most promising and efficient alternatives [10], and it has already found widespread use due to its ease of installation and lack of emissions. Solar energy, for example, is a common and important choice in hybrid energy systems to improve power supply reliability and efficiency [11], and it has been successfully integrated with hydrogen [12], battery storage [13], diesel technologies [14], and other technologies.

Due to the exponential development of energy consumption, renewable energy sources (RESs) are critical for global energy systems. Solar power is a key renewable energy source for electrical energy generation. Furthermore, because of their benefits over conventional fossil fuels, RESs have grown popular for electrical power generation [15]. When compared to fossil fuels, the cost of RES for energy is zero, and the cost of maintenance is quite cheap. Furthermore, unlike fossil fuels, the accompanying CO2 emissions are zero. Studies have concentrated on increasing new methods to transform solar energy into electrical energy as a result of these factors. Solar photovoltaic (PV) cells serve as a conversion medium for solar energy to electrical energy. Because such systems demand more initial capital, defined studies are required to create a PV system for best utilization. To analyze and regulate a PV module, accurate PV system modelling is required [16]. The precise calculation of PV module parameters is a milestone in PV system exact modelling. Depending on the level of accuracy required, a solar PV module can be represented by one, two, or more diodes. The PV cell model is represented by electrical circuits with lumped parameter series resistance (R_s) and shunt resistance (R_{sh}) values [17], [18]. The three major models for modeling solar PV cells are the single-diode model (SDM), double-diode model (DDM), and three-diode model (PVM). Because of its suitable level of precision in terms of current–voltage (I–V) characteristics, the SDM is widely used. The SDM and DDM, respectively, have five and seven unknown parameters. The DDM, in comparison to the SDM, can more accurately denote a PV cell. The PVM model is unpopular because it contains nine unknown factors, and its design complexity grows as one additional diode is added to improve the model's accuracy [19]. The PV cells have nonlinear I-V curves, and the modelling equations are transcendental equations. Analytical approaches, numerical methods, and evolutionary algorithms are three types of methods for resolving nonlinear equations that have been documented in the literature [20]. Analytical methods can swiftly solve linear equations, but they may fail to solve nonlinear equations with multiple unknowns because complex problems demand more acceptable assumptions. When there are several unknowns, analytical procedures produce erroneous results. To discover the unknown parameters in analytical approaches, it is necessary to manipulate model equations mathematically. [21].

For solving nonlinear equations, numerical methods need the manufacturer's datasheet values along with some assumptions. Nonlinear equations are solved by utilizing iterative strategies in these methods. The most difficult aspect of such methods is estimating the beginning value, which has an impact on the solution's convergence rate. To solve nonlinear equations, the Gauss–Seidel (GS) and Newton–Raphson (NR) methods are commonly utilized [22], [23]. The NR method's convergence rate is quadratic in nature, and it has the highest convergence rate with the fewest iterations. Numerical methods are, in general, local search methodologies. Several strategies for extracting parameters of lumped electrical circuit models of PV cells based on data sheet information or observed I-V data are widely accessible. Analytical procedures, also known as direct techniques, are methods for estimating parameters based on the direct solution of empirical relationships between distinct factors. Some methods employ the Lambert-W function to estimate parameters [24]. Analytical approaches, in general, compute PV cell model parameters in a single iteration. These methods are aimed at constructing empirical relationships between various PV cell characteristics and solving those using V_{oc}, I_{sc}, and MPP values at Standard Test Conditions (STC). Because of the non-linear character of equations, various assumptions must be made in order to solve them using algebraic procedures [25]. As a result, analytical approaches can be applied with minimal computing and financial constraints, but with lower precision [26]. In fact, the accuracy of analytical techniques is heavily reliant on the accuracy of data sheet information. Reduced form based analytical approaches have been proposed to address the drawbacks of traditional analytical techniques. These methods are intended to limit the number of equations that need to be solved, and therefore the search space, in order to increase convergence and accuracy. These strategies are well-suited for SDM, but their applicability for DDM has yet to be determined. Numerical approaches, on the other hand, use an iterative or repeating procedure to estimate PV cell parameters. Empirical relational equations between parameters are established at significant locations on the I-V curve, such as axes intercepting points and MPP, in the same way as analytical approaches are. The influence of T and G on the I_{ph}, I_{sh}, R_s, R_{sh}, and n is analyzed to produce these empirical equations [27]. Numerical approaches such as the Newton-Raphson method, Gaussian iteration method, and non-linear least square method were used to solve these equations. As a result, the accuracy of parameter estimates using numerical approaches is determined by the fitting algorithm used, the objective function provided by the user, and the initial guess [27], [28]. Despite the fact that numerical approaches can yield PV cell parameters with more accuracy than analytical methods, there are some inherent limitations. First, numerical approaches' convergence is highly dependent on the initial solution guess. Second, using gradient operations complicates the solution process, and the singularity condition may arise during this approach.

Recently, meta-heuristic optimization methods have been widely used to estimate the parameters of PV cells in order to overcome the limitations of numerical methodologies. These algorithms are developed based on the evolutionary concept, biological behavior, and physical phenomena [29]–[33].

Improved convergence, immunity from initial guess, lack of singularity condition, and examination of all I-V data points rather than crucial places on the I-V curve are all advantages of meta-heuristic optimization techniques [34]. Various meta-heuristics optimization techniques have been utilized in the literature to acquire PV cell parameters. Some of these techniques include: Genetic Algorithms (GA) [35], Particle Swarm Optimization (PSO) [36], [37], Simulated Annealing (SA) [38], Harmony Search (HS) [39], Bacterial Foraging Algorithm (BFA) [40], [41], Teaching-Learning Based Optimization (TLBO) [42], Cuckoo Search algorithm (CSA) [43], Cat Swarm Optimization (CSO) [44], Differential Evolution (DE) [45], Whale Optimization Algorithm (WOA) [46], JAYA Optimization Algorithm (JAYA) [47], Firefly algorithm (FA) [48], [49], Artificial Bee Colony (ABC) [50], Gravitational Search Algorithm (GSA) [51], [52], Grey Wolf optimization (GWO) [43], Moth-Flame Optimization (MFO) [53]–[55] and Tunicate Swarm Algorithm (TSA) [56], Chaotic Inertia Weight Particle Swarm Optimization (CIWPSO) [57], artificial hummingbird algorithm (AHA) [58] and Flower Pollination Algorithm (FPA) [59], [60].

The rate of convergence, precision, and implementation complexity are all important factors to consider when choosing these optimization approaches. Although all of these methods have been shown to be accurate for parameter estimate, they each have their own set of limitations, such as the number of essential parameters that must be established, the complexity of the implementation, and the computational time necessary to complete the estimation. Research is underway to develop efficient algorithms to predict parameters of PV cells under different environmental conditions in the hunt for simple and faster techniques. Despite the fact that metaheuristic algorithms can produce acceptable results, no algorithm can outperform others in solving all optimization issues. As a result, various studies have been conducted to increase the performance and efficiency of the original metaheuristic algorithms and adapt them to a specific application.

These algorithms have attained remarkably good results when estimating the parameters of PV systems. However, it has to be pointed out that most of the above algorithms have to use additional parameters, except for the population size. The parameter settings greatly influence the performance of these algorithms. Setting the proper parameter values for a specific problem is still challenging. The parameter tuning is also a tedious task. Therefore, developing a competitive and advanced algorithm to extract the parameters of these models is still demanding work.

Tunicate Swarm Algorithm (TSA) is a recently developed bioinspired meta-heuristic optimization technique that is firstly proposed by Kaur *et al.* [61]. Tunicates employ swarm intelligence and jet propulsion at sea to find the best state in their environment for finding food. TSA is better than other competitive methods at finding optimal solutions and is suitable for tackling real-world optimization problems. However, it suffers from getting trap in local optima and couldn't converge to a best solution for some complex cases [62].

In order to overcome this weakness, an improved version of the tunicate swarm algorithm (ITSA) is developed and utilized for parameter identification of photovoltaic systems in the current study. According to the ''No free lunch theory'', there is no metaheuristic algorithm providing a superior performance than others in solving all optimizing problems [63]. By far, no universal methods are found to be suitable for all the problems. In other words, one method may produce satisfying solutions for some particular problems but fail to achieve it in other problems. As a result, it is of great importance to further develop some new and effective metaheuristic methods for real-world problems with unknown decision spaces. Motived by this practical necessity, this research successfully develops ITSA and utilized it for parameter identification of photovoltaic systems. The major contributions of this study are as follows:

- Introducing a novel algorithm called ITSA with the purpose to enhance the behavior of tunicates in the TSA.
- Introducing a new phase in TSA to pick a candidate solution at random instead of the best solution to increase the exploration and allows the TSA algorithm to perform a more powerful global search all around the search space.
- Investigation the effectiveness of ITSA algorithm for parameter extraction of different PV models, single-diode, double-diode, and PV module. A parameter perturbation approach is proposed to validate these algorithms for solving parameter estimation issues using I-V data. In addition, statistical analysis was performed over 100 trials to compare the effectiveness of these algorithms with existing algorithms.
- Comparing the performance of ITSA for global optimization with swarm intelligence (SI) algorithms such as GSA, GWO, and SCA.

The results prove that the ITSA has the capability to improve the performance of the original TSA with better solutions and a fast convergence rate.

The rest of the paper is organized as follows: Section 2 introduces the mathematical equation formulation for parameter evaluation of PV models is presented. Sections 3 and 4 explain the proposed modified optimization algorithm. The comparative time complexity analysis is explained in section 5. The Performance evaluation of the ITSA is presented in section 6. Section 7 exhibits the experimental results and discussion. Section 8 discusses the conclusion and future work.

II. MATHEMATICAL MODELING & PROBLEM STATEMENT OF PV

Many models exist in the relevant publications to describe the physical PV cell's features. The SDM and the DDM are two of the most commonly used equivalent circuit mathematical

models to define the nonlinear features of PV systems. The mathematical formulas for the three different PV models (SDM, DDM, and PVM), as seen in Fig. 1, are described in this section. This section also covers the objective function. [39], [64].

A. SDM

Because of its simple form and precision, the SDM is frequently used to illustrate the static features of solar cells. The SDM is made up of a diode, a current source, a shunt resistor, and a series resistor, as shown in Fig. 1. (a). It's worth mentioning that the shunt and series resistors are used to indicate leakage current and load current loss, respectively. To account for the contact resistance between silicon and electrode surfaces, electrode resistances, and current flow resistances, they're all modelled as R_s. In addition, R_{sh} is used to account for the leakage current of a P-N junction diode. As a result, the SDM has five parameters: I_{ph}, I_{sd}, n, R_s, and R_{sh}. The SDM's I-V characteristics are given by Eq. (1) [26].

$$I_L = I_{ph} - I_{sd}\left(exp\left(\frac{V_L + R_s I_L}{n\frac{kT}{q}}\right) - 1\right) - \frac{V_L + R_s I_L}{R_{sh}} \quad (1)$$

where I_{sd} denotes the diode's saturation current; and V_L and I_L denote the measured I-V data acquired from the PV cell. R_s denotes series resistance; q and k denote electron charge ($1.60217646 \times 10^{-19}$C) and Boltzmann constant ($1.3806503 \times 10^{-23}$ J/K), respectively; n denotes diode ideal factor; T denotes cell temperature (K); R_{sh} stands for shunt resistance. The photovoltaic effect causes current to flow through the P-N junction, which is referred to as I_{ph}, in the presence of irradiance.

It can be seen that there are five unknown parameters in SDM that need to be retrieved (I_{ph}, I_{sd}, n, R_s *and* R_{sh}).

B. DDM

The effect of recombination current loss in the depletion area has been integrated into DDM to improve the accuracy of the PV cell circuit model offered in SDM. A second diode is added to represent current loss in the depletion area. As a result, at low irradiance levels, the DDM model is more accurate. This extra diode, however, adds two new parameters: n and I_{sd}. The DDM's circuit model is shown in Fig. 1. (b). Equation (2) can be used to obtain the DDM's I-V characteristics.

$$I_L = I_{ph} - I_{sd1}\left(exp\left(\frac{V_L + R_s I_L}{n_1\frac{kT}{q}}\right) - 1\right) - I_{sd2}\left(exp\left(\frac{V_L + R_s I_L}{n_2\frac{kT}{q}}\right) - 1\right) - \frac{V_L + R_s I_L}{R_{sh}} \quad (2)$$

where I_{s1} and n_1 stand for diffusion current and ideality factor, respectively; n_2 and I_{s2} stand for composite diode ideality factor and saturation current, respectively. As a result, the DDM model comprises seven parameters that must be precisely extracted: I_{ph}, I_{sd1}, n_1, I_{sd2}, n_2, Rs and R_{sh}.

C. PVM

To form a PVM, PV cells are linked in series or parallel, depending on the voltage and current requirements. Fig. 1. (c) shows the comparable circuit schematic for the single diode PVM. Formula (3) can be used to compute the output current of this model [64], [65].

$$I_L = I_{ph}N_p - I_{sd}N_p\left(exp\left(\frac{V_L + R_s I_L N_s/N_p}{nN_s\frac{kT}{q}}\right) - 1\right) - \frac{V_L + R_s I_L N_s/N_p}{R_{sh}N_s/N_p} \quad (3)$$

where N_s and N_p denote the number of solar cells connected in series or parallel, respectively. N_p is set to 1 because the *PVM* used in this study are all in series. As a result, Eq. (3) can be written as follows:

$$I_L = I_{ph} - I_{sd}\left(exp\left(\frac{V_L + R_s I_L N_s}{nN_s\frac{kT}{q}}\right) - 1\right) - s\frac{V_L + R_s I_L N_s}{R_{sh}N_s} \quad (4)$$

There are five unknown parameters for the PVM (I_{ph}, I_{sd}, n, R_s *and* R_{sh}) that must be extracted.

D. PROBLEM FORMULATION

The parameter identification problem must identify the minimal error value by measuring and simulating I-V data under various lighting temperatures and other environmental circumstances in order to find the ideal parameter value. To make use of optimization algorithms, parameter extraction issues are typically turned into a class of optimization problems. In the table's last row, the root mean square error (RMSE) is the objective function used to evaluate the overall difference between measured and simulated current data. The RMSE is employed as the objective function in this study, as it is in [20], and it is defined as follows:

$$RMSE\ (\boldsymbol{X}) = \sqrt{\frac{1}{M}\sum_{d=1}^{M} f\ (V_L.I_L.\boldsymbol{X})^2} \quad (5)$$

$\boldsymbol{X}$ is a vector that concludes the unknown parameters to be retrieved, and M is the number of measured I-V data. As a result, the error function values $f\ (V_L.I_L.\boldsymbol{X})$ of SDM, DDM, and PVM for various PV models can be represented as follows:

- For SDM:

$$f\ (V_L.I_L.\boldsymbol{X}) = I_{ph} - I_{sd}\left(exp\left(\frac{V_L + R_s I_L}{n\frac{kT}{q}}\right) - 1\right) - \frac{V_L + R_s I_L}{R_{sh}} - I_L$$
$$\boldsymbol{X} = \left\{I_{ph}.I_{sd}.R_s.R_{sh}.n\right\} \quad (6)$$

• For SDM:

$$\begin{cases} f\left(V_L.I_L.\boldsymbol{X}\right) = I_{ph} - I_{sd1}\left(exp\left(\dfrac{V_L + R_s I_L}{n_1 \frac{kT}{q}}\right) - 1\right) \\ \qquad\qquad - I_{sd2}\left(exp\left(\dfrac{V_L + R_s I_L}{n_2 \frac{kT}{q}}\right) - 1\right) \\ \qquad\qquad - \dfrac{V_L + R_s I_L}{R_{sh}} - I_L \\ \boldsymbol{X} = \left\{I_{ph}.I_{sd1}.I_{sd2}.R_s.R_{sh}.n_1.n_2\right\} \end{cases} \tag{7}$$

• For PVM:

$$\begin{cases} f\left(V_L.I_L.\boldsymbol{X}\right) = I_{ph} - I_{sd}\left(exp\left(\dfrac{V_L + R_s I_L N_s}{n N_s \frac{kT}{q}}\right) - 1\right) \\ \qquad\qquad - \dfrac{V_L + R_s I_L N_s}{R_{sh} N_s} - I_L \\ \boldsymbol{X} = \left\{I_{ph}.I_{sd}.R_s.R_{sh}.n\right\} \end{cases} \tag{8}$$

III. TUNICATE SWARM ALGORITHM

Tunicate swarm algorithm (TSA) is a relatively simple meta-heuristic optimization technique inspiration by the performance of marine tunicates and their jet propulsion systems during navigation and foraging [61]. This animal has a millimeter-scale form. Tunicate can locate food sources in the sea. In the supplied search space, however, there is no indication of the food source. When traveling with a jet propulsion behavior, a tunicate must meet three fundamental conditions: (i) it must avoid confrontation with other tunicates in the search space, (ii) it must take the right path to the best search location, and (iii) it needs to be as near to the finest search agent as feasible. The candidate solutions (i.e. tunicates) in TSA are looking for the best food source (i.e. the best value of the objective function). In this process, the tunicates update their positions in relation to the best tunicates that are stored and enhanced in each iteration. The TSA begins with the population of randomly generated tunicates considering the permissible bounds of the design variables according to the following equation:

$$\vec{T}_p = \vec{T}_p^{min} + rand \times \left(\vec{T}_p^{max} - \vec{T}_p^{min}\right) \tag{9}$$

where, $\vec{T}_p$ is the position of each tunicate and *rand* is a random number within range [0,1]. $\vec{T}_p^{min}$ and $\vec{T}_p^{max}$ are minimum and maximum values of design variables, respectively. During the iterations, the tunicates update their position through the following formula [61]:

$$\vec{T}_p\left(\vec{x}+1\right) = \frac{\vec{T}_p\left(x\right) + \vec{T}_p\left(\vec{x}\right)}{2 + c_1} \tag{10}$$

where, c_1 is a random number within range [0,1] and $\vec{T}_p\left(x\right)$ refers to the updated position of the tunicate with respect to the position of the food source based on Eq. (11).

$$\vec{T}_p\left(x\right) = \begin{cases} SF + A \times \left|SF - rand \times \vec{T}_p\right|, & if\ rand \geq 0.5 \\ SF - A \times \left|SF - rand \times \vec{T}_p\right|, & if\ rand < 0.5 \end{cases} \tag{11}$$

where *SF* is the food source, which is represented by the population's optimal tunicate position; and *A* denotes a randomized vector to prevent tunicates from colliding with one another which is modelled as:

$$A = \frac{c_2 + c_3 - 2c_1}{VT_{min} + c_1\left(VT_{max} - VT_{min}\right)} \tag{12}$$

where, c_1, c_2 and c_3 are random numbers within range [0,1]; VT_{min} and VT_{max} reflect the minimum and maximum speeds that are used to create social interaction which considered as 1 and 4, respectively [61].

The TSA algorithm's steps are presented below:

Step 1: Initialize the tunicate population $\vec{T}_p$ based on Eq. (9).

Step 2: Choose the initial parameters and maximum number of iterations.

Step 3: Calculate the fitness value of each search agent.

Step 4: The best tunicate is explored in the given search space.

Step 5: Update the position of each tunicate using Eq. (11).

Step 6: Adjust the updated tunicate which goes beyond the boundary in a given search space.

Step 7: Compute the updated tunicate fitness value. If there is a better solution than the previous optimal solution, then update the best.

Step 8: If the stopping criterion is satisfied, then the algorithm stops. Otherwise, repeat the Steps 5–8.

Step 9: Return the best optimal solution which is obtained so far.

IV. MODIFIED TUNICATE SWARM ALGORITHM

Despite the TSA's ability to produce efficient results when compared to other well-known algorithms, it is susceptible to becoming trapped in local optima and is not ideal for very complex problems with several local optima [62]. As shown in Eqs. (10) and (11), In TSA, every tunicate update its position based on the position of food source (i.e. position of the best tunicate in the whole population). It means that at each iteration pass, the TSA algorithm updates the position of candidate solutions around a single point. However, without any knowledge of the position of the food source (FS), there will not be any recovery for the algorithm if premature convergence happens. In other words, once the algorithm has converged, it loses its potential to explore and becomes inactive. Therefore, the TSA algorithm becomes locked at local minimum points as a result of this mechanism. In light of these conditions, ITSA is proposed to overcome the mentioned weakness and to increase the search capability and flexibility of the algorithm.

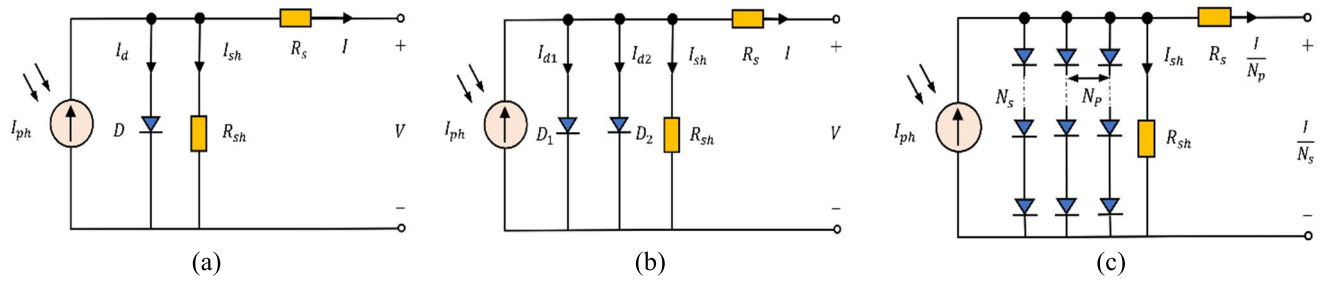

FIGURE 1. Schematic of PV cell models (a) SDM (b) DDM (c) PVM.

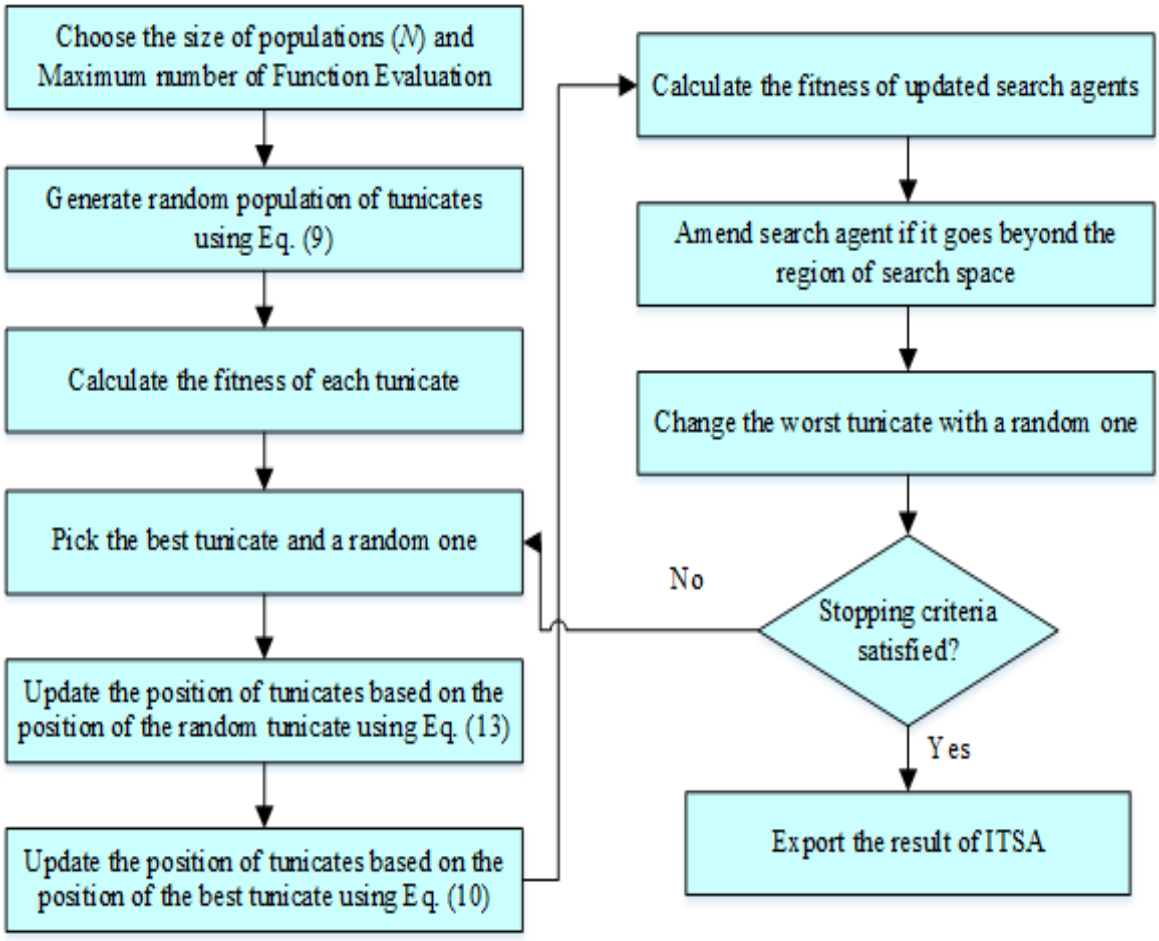

FIGURE 2. Flowchart of the ITSA.

Generally, exploration and exploitation are two key features to the success of any meta-heuristic algorithm and they need to be designed effectively. The exploration is the ability of expanding global investigation of the search space, where the exploitation is the ability of finding the optima around a good solution. In the proposed ITSA, the original algorithm is modified to increase its exploration and exploitation capability.

In order to improve the performance and exploration ability of the algorithm, the proposed ITSA has two main phases in each iteration. In the first phase, a candidate solution is picked at random instead of the best solution and the position of the candidate solutions will be updated according to the position of this random tunicate. This procedure encourages exploration and allows the TSA algorithm to perform a more powerful global search all around the search space. The exploration phase of the ITSA is mathematically modeled as follows:

$$\vec{T}_p(\vec{x}+1) = \vec{T}_p(r) - rand \times |\vec{T}_p(r) - 2rand \times \vec{T}_p(\vec{x})| \quad (13)$$

where $\vec{T}_p(r)$ is randomly selected tunicate form the current population.

TABLE 1. Description of benchmark functions.

Function	Range	f_{min}
$F_1(X) = \sum_{i=1}^{n} x_i^2$	$[-100, 100]^n$	0
$F_2(X) = \sum_{i=1}^{n} \lvert x_i \rvert + \prod_{i=1}^{n} \lvert x_i \rvert$	$[-10, 10]^n$	0
$F_3(X) = \sum_{i=1}^{n} \left(\sum_{j=1}^{i} x_j \right)^2$	$[-100, 100]^n$	0
$F_4(X) = \max_i \{ \lvert x_i \rvert, 1 \le i \le n \}$	$[-100, 100]^n$	0
$F_5(X) = \sum_{i=1}^{n-1} \left[100(x_{i+1} - x_i^2)^2 + (x_i - 1)^2 \right]$	$[-30, 30]^n$	0
$F_6(X) = \sum_{i=1}^{n} -x_i \sin(\sqrt{\lvert x_i \rvert})$	$[-500, 500]^n$	$428.9829 \times n$
$F_7(X) = \sum_{i=1}^{n} [x_i^2 - 10\cos(2\pi x_i) + 10]$	$[-5.12, 5.12]^n$	0
$F_8(X) = -20 \exp\left(-0.2 \sqrt{\frac{1}{n} \sum_{i=1}^{n} x_i^2} \right) - exp\left(\frac{1}{n} \sum_{i=1}^{n} \cos(2\pi x_i) \right) + 20 + e$	$[-32, 32]^n$	0
$F_9(X) = \frac{1}{4000} \sum_{i=1}^{n} x_i^2 - \prod_{i=1}^{n} \cos\left(\frac{x_i}{\sqrt{i}} \right) + 1$	$[-600, 600]^n$	0
$F_{10}(X) = \frac{\pi}{n} \{ 10 \sin(\pi y_1) + \sum_{i=1}^{n-1} (y_i - 1)^2 [1 + 10 \sin^2(\pi y_{i+1})] + (y_n - 1)^2 \} + \sum_{i=1}^{n} u(x_i, 10, 100, 4)$	$[-50, 50]^n$	0
$y_i = 1 + \frac{x_{i+4}}{4}$ $\quad u(x_i, a, k, m) = \begin{cases} k(x_i - a)^m & x_i > a \\ 0 & a < x_i < a \\ k(-x_i - a)^m & x_i < -a \end{cases}$		

TABLE 2. Bound setting of the proposed methods.

year	Algorithm	Parameter	Specifications
2022	ITSA	Search agents	40
		Parameter VTmin	1
		Parameter VTmax	4
		Maximum iteration number	1000
2020	TSA	Search agents	80
		Parameter $Pmin$	1
		Parameter $Pmax$	4
		Maximum iteration number	1000
2016	SCA	Search agents	80
		Number of elites	2
		Maximum iteration number	1000
2009	GSA	Search agents	80
		Gravitational constant	100
		Alpha coefficient	20
		Maximum iteration number	1000
2014	GWO	Search agents	80
		Control parameter ($\vec{a}$)	[2,0]
		Maximum iteration number	1000

In the second phase of the ITSA algorithm, the tunicates update their position according to the position of the best tunicate based on Eq. (10) to explore the near-optimal positions and constructive movement toward the global best solution. Furthermore, in the proposed ITSA, the worst tunicate with the highest objective function value will be replaced with a randomly generated tunicate at each iteration. Figure 2 shows the flowchart of the proposed ITSA algorithm.

V. COMPARATIVE TIME COMPLEXITY ANALYSIS

The time complexity analysis of most algorithms involves analyses of three components. Likewise, the time complexity

TABLE 3. Results comparison of different algorithms in solving test functions.

Function	Statistics	ITSA	TSA	SCA	GSA	GWO
F_1	Best	**0.00**	5.1458e-61	1.5523e-07	1.0013e-17	2.4915e-61
	Worst	**0.00**	1.1586e-54	0.0043	3.1868e-17	3.8647e-58
	Mean	**0.00**	8.3155e-56	2.3458e-04	2.1148e-17	4.9162e-59
	Std.	**0.00**	2.4905e-55	7.9295e-04	5.8150e-18	1.0230e-58
F_2	Best	**0.00**	1.1196e-35	1.5005e-09	1.5282e-08	8.3612e-36
	Worst	**0.00**	3.2814e-32	9.8446e-06	3.3313e-08	5.3488e-34
	Mean	**0.00**	2.1532e-33	1.6882e-06	2.3935e-08	8.3658e-35
	Std.	**0.00**	6.0237e-33	2.4046e-06	4.0025e-09	9.8594e-35
F_3	Best	**0.00**	2.5684e-32	70.8285	102.9550	1.2533e-19
	Worst	**0.00**	2.4492e-17	2.6762e+03	468.6160	3.5572e-13
	Mean	**0.00**	8.1741e-19	789.1620	245.4694	1.5096e-14
	Std.	**0.00**	4.4714e-18	746.2287	100.1024	6.5547e-14
F_4	Best	**0.00**	3.2458e-08	1.2610	2.2498e-09	9.8174e-16
	Worst	**0.00**	6.3429e-05	35.6743	5.0857e-09	2.4431e-13
	Mean	**0.00**	1.0102e-05	9.3080	3.3030e-09	1.9487e-14
	Std.	**0.00**	1.6927e-05	8.0720	7.4424e-10	4.4955e-14
F_5	Best	**0.122**	25.6273	27.3230	25.7459	25.2273
	Worst	**8.171**	29.5430	49.5110	220.9110	28.7294
	Mean	**2.337**	28.4422	29.9106	42.2647	26.9256
	Std.	**2.772**	0.7616	4.1508	45.4674	0.8418
F_6	Best	**-1.2569e+04**	-7.8992e+03	-5.2993e+03	-3.6279e+03	-8.8178e+03
	Worst	**-1.2563e+04**	-5.2761e+03	-3.5321e+03	-2.0033e+03	-4.9742e+03
	Mean	**-1.2568e+04**	-6.6126e+03	-4.0769e+03	-2.7826e+03	-6.2524e+03
	Std.	**1.864**	599.2609	336.8249	365.4671	852.4634
F_7	Best	**0.00**	77.7761	1.0560e-06	8.9546	0.00
	Worst	**0.00**	254.9883	51.4451	21.8891	10.0548
	Mean	**0.00**	151.4539	5.9694	15.6209	0.8853
	Std.	**0.00**	35.8717	12.2476	3.1043	2.4438
F_8	Best	**8.8818e-16**	1.5099e-14	1.5579e-05	2.5288e-09	1.1546e-14
	Worst	**8.8818e-16**	4.3125	20.2198	4.4823e-09	2.2204e-14
	Mean	**8.8818e-16**	2.4095	14.3622	3.4912e-09	1.5928e-14
	Std.	**0.00**	1.3920	8.9778	5.1530e-10	2.5861e-15
F_9	Best	**0.00**	0.00	4.8381e-07	1.6952	0.00
	Worst	**0.00**	0.0159	0.7703	10.6642	0.0140
	Mean	**0.00**	0.0077	0.1368	4.2510	0.0014
	Std.	**0.00**	0.0057	0.2218	2.0234	0.0041
F_{10}	Best	2.168e-06	0.2738	0.2631	**8.2033e-20**	0.0121
	Worst	**0.0022**	13.8088	5.6300	0.1037	0.0920
	Mean	**6.989e-04**	6.3735	0.9568	0.0198	0.0364
	Std.	**6.822e-04**	3.4586	1.1497	0.0400	0.0201

analysis of ITSA also requires analyses of these three components:

1. Time complexity of initialization of the population, generally bounded by $\Phi(n \times d)$ where n denotes the population size and d denotes the dimensions/design variables of the problem
2. Time complexity of initial fitness evaluation, generally bounded by $\Phi(n \times C_{0bj})$, where C_{obj} represents the cost of the objective function.
3. Time complexity of the main loop, generally bounded by $\Phi(Maxiterations \times (n \times d + n \times C_{0bj}))$, where $Maxiterations$ is the maximum number of iterations.

Hence, the total time complexity of ITSA algorithm is $\Phi(Maxiterations(n \times d + n \times C_{0bj}))$.

VI. PERFORMANCE EVALUATION OF THE ITSA

In this section the effectiveness verification of the proposed ITSA method will be investigated. To this aim, the performance of the new algorithm is compared with the standard version of the algorithm (TSA) as well as some well-known metaheuristic algorithms on a collection of benchmark test functions from the literature. These are all minimization problems that can be used to assess the robustness and search efficiency of new optimization algorithms. Table 1 shows the mathematical formulation and features of these test functions.

The ITSA algorithm's performance is compared with original TSA and some efficient optimization methods include GSA, GWO, and SCA. It's worth noting that the ITSA algorithm evaluates the objective function twice per iteration, whereas the TSA and other approaches do so just once. Therefore, to have fair comparison between the results, the size of population (N) is considered equal to 40 for ITSA and equal to 80 for TSA and other approaches. In addition, for all techniques, the maximum number of iterations are considered equal to 1000.

In this way, the same number of function evaluations equal to 80,000 is considered in all experiments. Because metaheuristics approaches are stochastic, the findings of a single run may be erroneous. As a result, statistical analysis

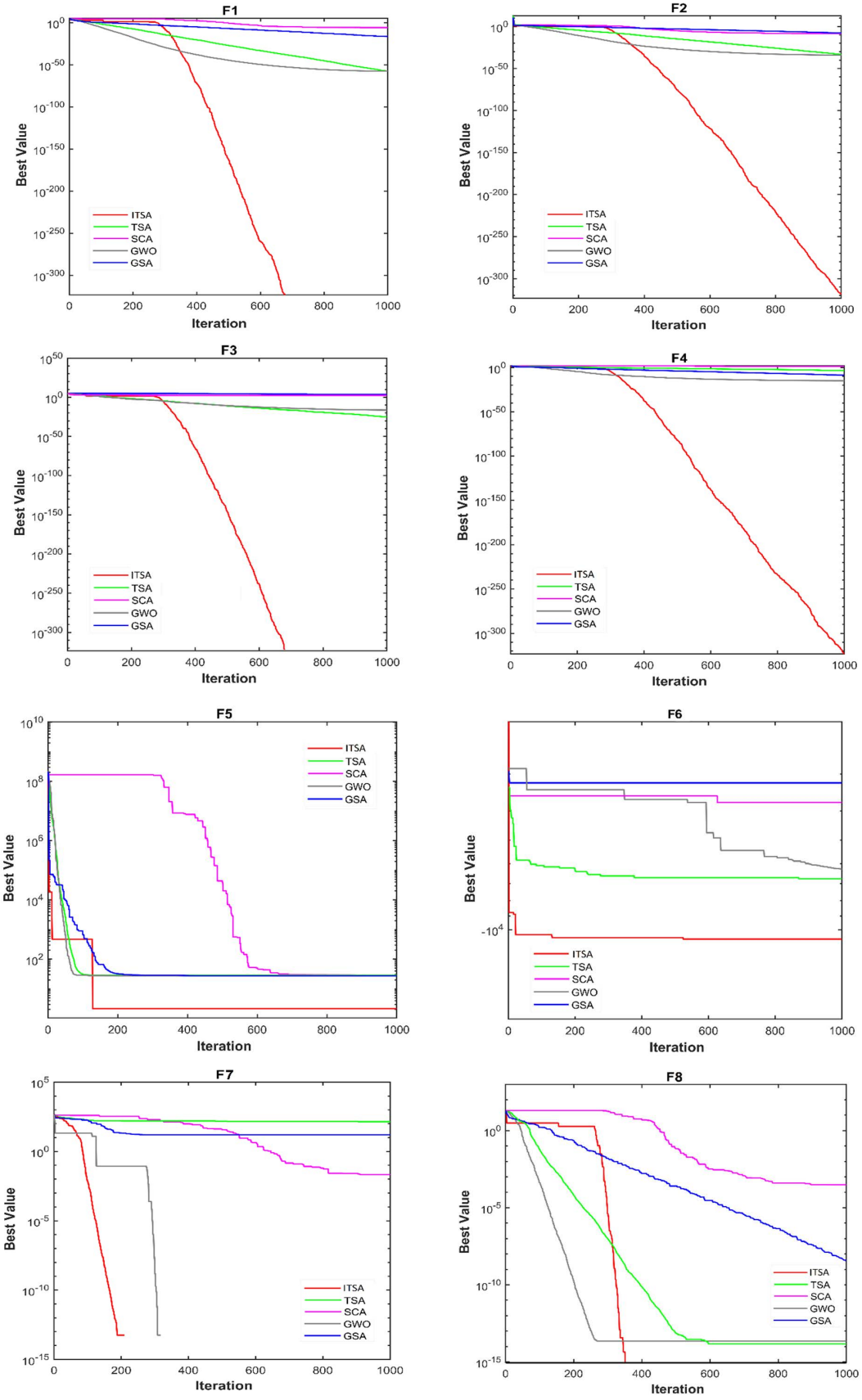

FIGURE 3. Convergence progress of the algorithms.

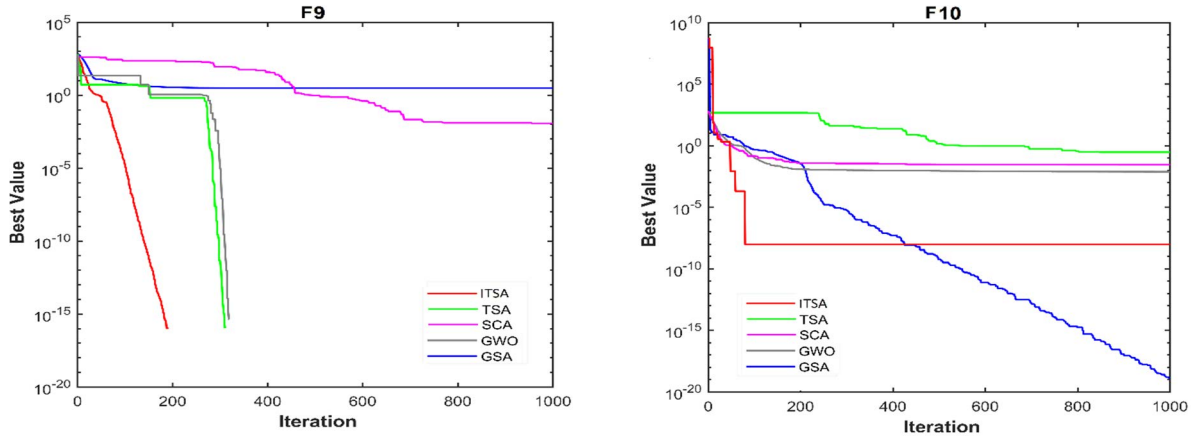

FIGURE 3. *(Continued.)* **Convergence progress of the algorithms.**

should be used to make a reasonable comparison and assess the algorithms' effectiveness. In order to address this issue, 30 separate runs are done for the specified algorithms and the results are presented in Tables 3.

Table 3 shows that, when compared to standard TSA and other optimization algorithms for all functions, ITSA could produce better solutions in terms of the best and mean value of the objective functions.

As shown in this Table, the new algorithm could converge to the global optimum for F_1, F_2, F_3, F_4, F_6, F_7 and F_9. In addition, for the other functions (i.e., F_5, F_8, F_{10}), the new method could provide better results compared with the other techniques. The results also reveal that the ITSA algorithm's standard deviations are substantially smaller than those of the other approaches, indicating the algorithm's stability. In Figure 3, for all benchmark test functions, the convergence progress curves of ITSA are compared to those of TSA and other approaches. As shown in this figure, the ITSA is capable of doing a full investigation of the search area and promptly identifying the most promising position. Based on the findings, it can be inferred that ITSA outperforms the original algorithm as well as alternative optimization methods. The parameters of the ITSA and other methods are presented in table 2. These parameters have been selected based on the suggestions presented in the original papers of each technique.

VII. EXPERIMENTS AND DISCUSSIONS

Based on the main objective of the current study, in this section the proposed ITSA algorithm is applied for parameter identification of PV models. In this subsection, three different solar PV models (SDM, DDM, and PVM) parameter extraction problems are solved using ITSA in order to further examine the effectiveness of the proposed ITSA. The SDM, DDM, and poly-crystalline Photowatt-PWP201 modules are the three models in issue. The 57 mm diameter commercial silicon RTC France is used to obtain the I-V data of the SDM and DDM [66]. At a temperature of 33 °C and an irradiance of 1000 W/m2, a silicon solar cell from France works. In addition, the Photowatt-PWP201 is used as a PVM to evaluate the ITSA and determine the associated parameters. [67], [68]. The Photowatt-PWP201, in particular, includes 36 silicon cells with series conductivity of less than 1000 W/m2 at 45 °C. The parameter search ranges for the three PV models are provided in Table 4 [69]–[71].

TSA, SCA, GSA, GWO, and PSO are five well-known meta-heuristic algorithms that are examined to validate the competitive performance of ITSA. On each PV model, all of the compared methods were run 30 times in a row. The maximum number of evaluations for the comparative methods is set to 50,000 for each execution. Furthermore, the accuracy of the six analyzed approaches was demonstrated by comparing their best RMSE values. Through the study of data results and convergence curves, their resilience and convergence speed were also assessed.

A. RESULTS ON THE SDM

Table 5 shows the ideal parameters extracted and the RMSE values for the SDM, with the best results shown in boldface when the RMSE is at its minimum. Table 4 shows that among the six algorithms, the ITSA has the best RMSE values (9.86E-04 and 1.16E-03, respectively); also, the GWO has the second best RMSE value (1.16E-03), followed by GSA, PSO, TSA, and SCA. Because correct parameter values are not accessible, the RMSE is used to indicate the accuracy of experimental results. Despite the small difference between the best and second best RMSE values, in the objective function, reducing the disparity between the true and estimated parameter values is crucial. Because the RMSE of the objective value is smaller, the estimated parameters are more accurate. In addition, the best parameters retrieved from ITSA are used to plot I-V and P-V curves. The SDM's I-V and P-V characteristic curves in Fig. 4 reveal that the computed data provided by ITSA closely matches the actual data, implying that the suggested technique is more accurate than conventional SDM algorithms. Fig. 5 shows the convergence curves of all algorithms over the entire process.

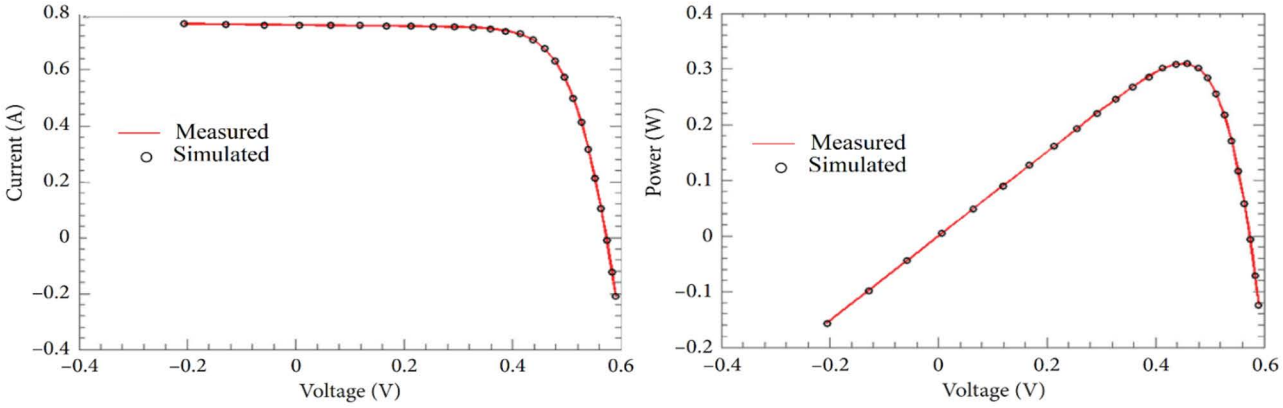

(a) *I-V* curve (b) *P-V* curve

FIGURE 4. The measured data and simulated data obtained by ITSA on SDM.

TABLE 4. Parameters boundaries of the three different photovoltaic (PV) models.

Parameter	***SDM/DDM***		***Photowatt-PWP201***	
	Lower Bound	***Upper Bound***	***Lower Bound***	***Upper Bound***
$I_{ph}(A)$	0	1	0	2
$I_{sd}, I_{sd1}, I_{sd2}(\mu A)$	0	1	0	50
$R_S(\Omega)$	0	0.5	0	2
$R_{sh}(\Omega)$	0	100	0	2000
n, n_1, n_2	1	2	1	50

TABLE 5. Comparison between algorithms on the SDM.

Algorithm	$I_{ph}(A)$	$I_{sd1}(\mu A)$	$R_S(\Omega)$	$R_{sh}(\Omega)$	n	*RMSE*
ITSA	0.7683	0.3262	0.0367	54.2557	1.4958	**9.86E-04**
TSA	0.7616	0.333	0.0370	56.874	1.4799	2.03E-03
SCA	0.7781	0.634	0.0361	100	1.546	2.19E-02
GSA	0.7607	0.05	0.0339	63.778	1.548	1.21E-03
GWO	0.7611	0.418	0.0354	57.138	1.507	1.16E-03
PSO	0.7383	0.319	0.0364	53.409	1.4799	1.43E-03

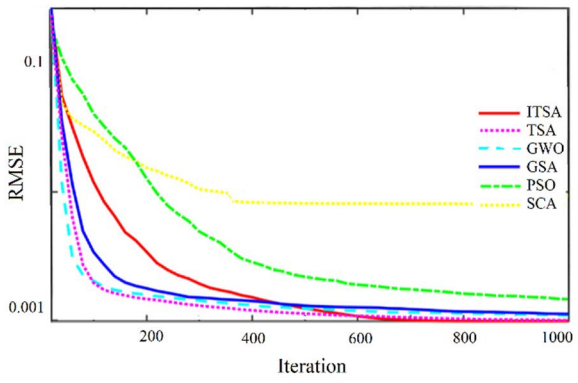

FIGURE 5. The convergence curves in the SDM.

B. DOUBLE DIODE MODEL

In comparison to the SDM, the DDM requires the identification of seven parameters. Although the number of parameters to be retrieved rises, it is thought to be more precise since the influence of the model's recombination current loss is taken into account. The retrieved parameters and RMSE values of the compared algorithms are shown in Table 6. Table 6 shows that among the six algorithms, only ITSA produced the best result (9.82E-04). The DDM's ideal RMSE value (9.82E04) is obviously smaller than the SDM's RMSE value (9.86E-04), confirming the DDM's accuracy. This also implies that as the number of factors increases, the performance of many algorithms to discover the best solution begins to deteriorate. Figure 6 shows a comparison of simulated and measured current and power values, similar to the SDM. The simulated current data agrees well with the measured current data, as shown in Fig. 6(a). The simulated power data and the measured power data in Fig. 6(b) support the same conclusion, indicating that RLDE continues to outperform the DDM. Fig. 7 shows the convergence curves of all algorithms over the entire process.

C. RESULTS ON THE PV MODULE MODEL

There are five parameters that must be estimated for the PVM. For each of the six examined approaches, Table 7 shows the best RMSE and the five extracted parameter values based on 30 tests. Table 7 shows that ITSA has the lowest RMSE

TABLE 6. Comparison between algorithms on the DDM.

Algorithm	$I_{ph}(A)$	$I_{sd1}(\mu A)$	$R_s(\Omega)$	$R_{sh}(\Omega)$	n_1	$I_{sd2}(\mu A)$	n_2	RMSE
ITSA	0.7608	0.9731	0.0369	53.8368	1.9213	0.1679	1.4281	**9.82E-04**
TSA	0.7610	0.197	0.03812	45.9993	1.4355	0.1388	1.7894	1.73E-03
SCA	0.7785	0.9741	0.03278	67.9366	1.5997	0.9569	1.6028	1.37E-02
GSA	0.7641	0.227	0.0344	39.780	1.9943	0.120	1.5492	2.03E-03
GWO	0.7635	0.11171	0.03672	52.9719	1.4142	0.3455	1.6184	1.02E-03
PSO	0.7676	0.13062	0.03588	51.1512	1.8145	0.3288	1.4858	2.90E-03

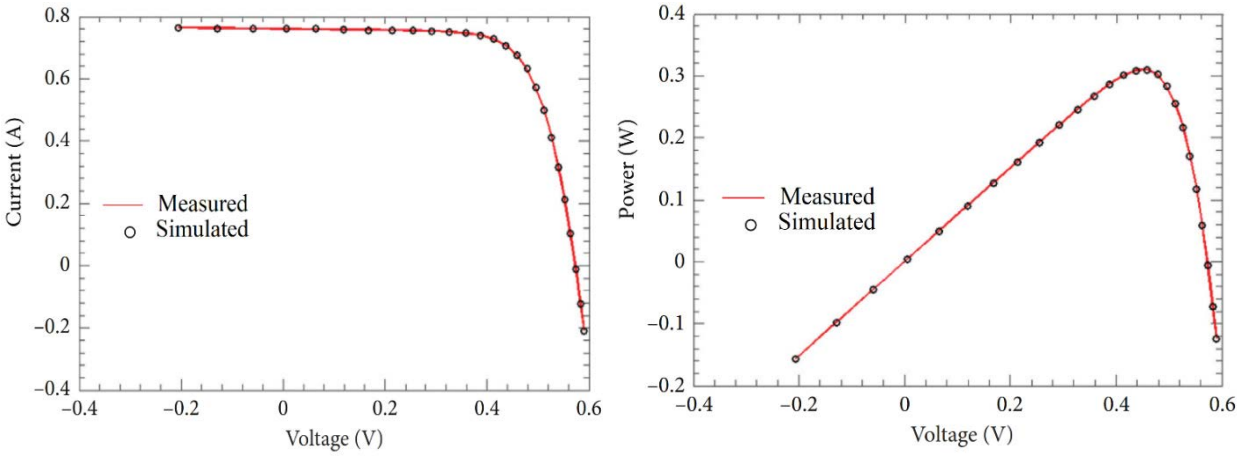

(a) *I-V* curve (b) *P-V* curve

FIGURE 6. The measured data and simulated data obtained by ITSA on DDM.

TABLE 7. Comparison between algorithms on the PVM model.

Algorithm	$I_{ph}(A)$	$I_{sd}(\mu A)$	$R_s(\Omega)$	$R_{sh}(\Omega)$	n	RMSE
ITSA	1.03185	3.28401	1.20556	841.321	48.4036	**2.427E-03**
TSA	0.7616	0.333	0.0370	56.874	1.4799	2.03E-03
SCA	1.0424	4.6816	1.2042	1204.0547	49.7875	1.03E-02
GSA	1.0309	3.7924	1.1889	946.2162	48.9771	2.46E-03
GWO	1.0284	4.9198	1.1650	1665.2265	50.0000	2.61E-03
PSO	1.0305	3.4904	1.2010	984.7794	48.6517	2.82E-03

value (2.42E-03), whereas the RSO has the highest RMSE value (2.42E-03) (2.44E-03). Furthermore, Fig. 8 indicates that the calculated parameters by ITSA have good I-V and P-V curve features that match the experimental values. Using this data, ITSA can extract parameters with high accuracy. Figure 8 shows that the simulated current (power) data provided by the proposed method is extremely compatible with the measured current (power) data, regardless of which modules are used. Table 6. There is a comparison among different algorithms on the PVM model. Fig. 9 shows the convergence curves of all algorithms over the entire process.

D. STATISTICAL RESULTS AND CONVERGENCE CURVES

The best value (Best), worst value (Worst), average value (Mean), and standard deviation (Std) of the method's RMSE value are also utilized to evaluate the overall performance of the proposed algorithm, in addition to the optimal parameters listed in the preceding subsection.

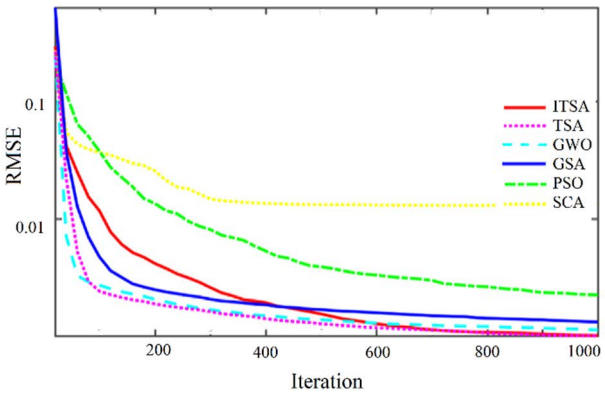

FIGURE 7. The convergence curves in the DDM.

A full comparison of the preceding algorithms is made in this subsection, and the statistical results are provided in Table 8, where some conclusions can be drawn. The dependability and convergence speed of the ITSA are

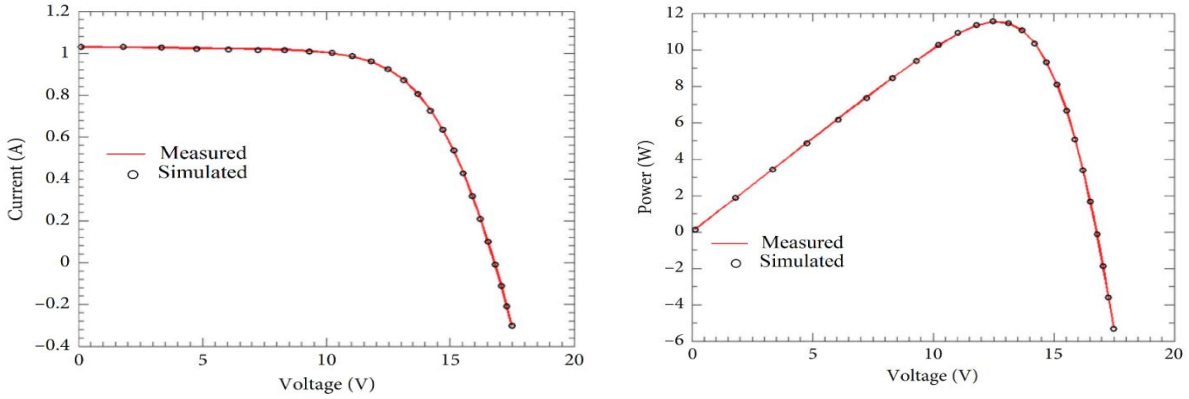

(a) *I-V* curve (b) *P-V* curve

FIGURE 8. The measured data and simulated data obtained by ITSA on PVM model.

TABLE 8. C comparison statistical results.

model	*Algorithm*	*RMSE*				
		Best	*Mean*	*Worst*	*Std*	*Sig.*
SDM	ITSA	**9.86E-04**	**9.89E-04**	**8.07E-03**	**3.01E-07**	+
	TSA	2.03E-03	2.64E-03	3.03E-03	2.23E-04	+
	GWO	1.16E-03	6.82E-03	4.51E-02	1.07E-04	+
	GSA	1.21E-03	1.81E-03	2.36E-03	2.51E-04	+
	PSO	1.43E-03	2.26E-03	2.87E-03	2.01E-04	+
	SCA	2.19E-02	4.28E-02	5.41E-02	6.84E-03	+
DDM	ITSA	**9.82E-04**	**9.80E-04**	**8.34E-03**	**1.45E-06**	+
	TSA	1.73E-03	2.19E-02	5.23E-02	2.29E-03	+
	GWO	1.02E-03	6.48E-03	3.83E-02	1.03E-03	+
	GSA	2.03E-03	2.87E-03	4.09E-03	3.63E-04	+
	PSO	2.90E-03	2.69E-03	3.54E-03	1.96E-04	+
	SCA	1.37E-02	4.54E-02	2.22E-01	3.49E-02	+
PVM	ITSA	**2.42E-03**	**2.43E-03**	**2.50E-03**	**1.38E-05**	+
	TSA	2.03E-03	1.73E-03	5.44E-02	3.29E-03	+
	GWO	2.61E-03	7.06E-02	2.75E-01	1.16E-01	+
	GSA	2.46E-03	2.61E-03	2.76E-03	5.99E-04	+
	PSO	2.82E-03	2.59E-03	3.46E-03	2.23E-04	+
	SCA	1.03E-02	1.28E-01	2.74E-01	1.07E-01	+

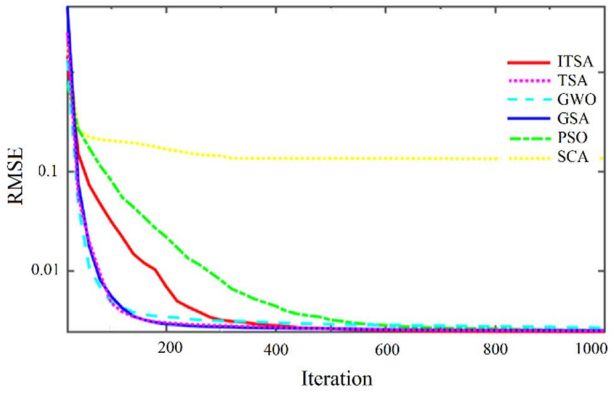

FIGURE 9. The convergence curves in the PVM module.

compared to the other six methods using convergence curves and statistical statistics.to see if there are any notable discrepancies between the outcomes obtained by the various methods. Table 8 displays the statistical results of the six methods across 30 separate tests on each of the three PV models, where the best, mean, worst, and standard values of RMSE represent the extracted parameters' accuracy, average precision, and dependability, respectively. To see if there are any notable discrepancies between the outcomes obtained by the various methods. A Wilcoxon signed-rank test with a significance level of 0.05 is used to compare the average results from 30 runs for each algorithm. The test results are shown in Table 8. All check symbols in Table 8 are '+,' indicating that there are significant differences in all test instances between ITSA and the comparison algorithms. Table 8 shows that the ITSA algorithm outperforms the other five algorithms in terms of model dependability and average accuracy. Furthermore, the results of the Wilcoxon signed-rank test in Table 8 show that ITSA outperforms all of the compared approaches on all three models.

VIII. CONCLUSION

In the optimization of PV systems, parameter extraction is crucial. This paper introduces ITSA, an improved optimization technique to retrieve parameters from photovoltaic models based on tunicate swarm optimization. ITSA is used to extract parameters from three photovoltaic models in order to test the performance of the suggested method. The experimental results show that the suggested ITSA outperforms the original TSA in terms of accuracy and reliability,

especially when compared to recent publications in the literature. Furthermore, the purpose of extracting photovoltaic model parameters is to improve the optimization and control of practical solar systems. The performance of proposed method has been assessed using parameter extraction problems from several PV models. The mean RMSE values generated by ITSA, are 9.84E−04, 9.82E−04, 2.42E−03 for SDM, DDM, and PVM, respectively. According to the experimental results, the solutions produced by the suggested ITSA are superior options for optimizing and managing real-world solar systems than the comparison algorithms. As a result, ITSA might be considered a good candidate technique for extracting parameters from other complex PV models.

REFERENCES

[1] B. Yang, T. Yu, H. Shu, Y. Zhang, J. Chen, Y. Sang, and L. Jiang, "Passivity-based sliding-mode control design for optimal power extraction of a PMSG based variable speed wind turbine," *Renew. Energy*, vol. 119, pp. 577–589, Apr. 2018.
[2] X. He, L. Chu, R. C. Qiu, Q. Ai, Z. Ling, and J. Zhang, "Invisible units detection and estimation based on random matrix theory," *IEEE Trans. Power Syst.*, vol. 35, no. 3, pp. 1846–1855, May 2020.
[3] K. Sun, W. Yao, J. Fang, X. Ai, J. Wen, and S. Cheng, "Impedance modeling and stability analysis of grid-connected DFIG-based wind farm with a VSC-HVDC," *IEEE J. Emerg. Sel. Topics Power Electron.*, vol. 8, no. 2, pp. 1375–1390, Jun. 2020.
[4] D. Song, Q. Chang, S. Zheng, S. Yang, J. Yang, and Y. H. Joo, "Adaptive model predictive control for yaw system of variable-speed wind turbines," *J. Mod. Power Syst. Clean Energy*, vol. 9, no. 1, pp. 219–224, 2021.
[5] J. Yang, L. Fang, D. Song, M. Su, X. Yang, L. Huang, and Y. H. Joo, "Review of control strategy of large horizontal-axis wind turbines yaw system," *Wind Energy*, vol. 24, no. 2, pp. 97–115, 2021.
[6] Z. Huang, B. Fang, and J. Deng, "Multi-objective optimization strategy for distribution network considering V2G-enabled electric vehicles in building integrated energy system," *Protection Control Mod. Power Syst.*, vol. 5, no. 1, pp. 1–8, Dec. 2020.
[7] H. Zhang, Z. Lu, W. Hu, Y. Wang, L. Dong, and J. Zhang, "Coordinated optimal operation of hydro–wind–solar integrated systems," *Appl. Energy*, vol. 242, pp. 883–896, May 2019.
[8] V. V. S. N. Murty and A. Kumar, "Multi-objective energy management in microgrids with hybrid energy sources and battery energy storage systems," *Protection Control Mod. Power Syst.*, vol. 5, no. 1, pp. 1–20, Dec. 2020.
[9] J. Liu, W. Yao, J. Wen, J. Fang, L. Jiang, H. He, and S. Cheng, "Impact of power grid strength and PLL parameters on stability of grid-connected DFIG wind farm," *IEEE Trans. Sustain. Energy*, vol. 11, no. 1, pp. 545–557, Jan. 2020.
[10] B. Yang, L. Jiang, L. Wang, W. Yao, and Q. H. Wu, "Nonlinear maximum power point tracking control and modal analysis of DFIG based wind turbine," *Int. J. Elect. Power Energy Syst.*, vol. 74, pp. 429–436, Jan. 2016.
[11] S. M. Mahmoudi, A. Maleki, and D. Rezaei Ochbelagh, "Optimization of a hybrid energy system with/without considering back-up system by a new technique based on fuzzy logic controller," *Energy Convers. Manage.*, vol. 229, Feb. 2021, Art. no. 113723.
[12] G. Zhang, Y. Shi, A. Maleki, and M. A. Rosen, "Optimal location and size of a grid-independent solar/hydrogen system for rural areas using an efficient heuristic approach," *Renew. Energy*, vol. 156, pp. 1203–1214, Aug. 2020.
[13] A. Maleki, M. A. Nazari, and F. Pourfayaz, "Harmony search optimization for optimum sizing of hybrid solar schemes based on battery storage unit," *Energy Rep.*, vol. 6, pp. 102–111, Dec. 2020.
[14] W. Cai, X. Li, A. Maleki, F. Pourfayaz, M. A. Rosen, M. A. Nazari, and D. T. Bui, "Optimal sizing and location based on economic parameters for an off-grid application of a hybrid system with photovoltaic, battery and diesel technology," *Energy*, vol. 201, Jun. 2020, Art. no. 117480.
[15] G. Xiong, J. Zhang, X. Yuan, D. Shi, Y. He, and G. Yao, "Parameter extraction of solar photovoltaic models by means of a hybrid differential evolution with whale optimization algorithm," *Sol. Energy*, vol. 176, pp. 742–761, Dec. 2018.
[16] R. Bendaoud, H. Amiry, M. Benhmida, B. Zohal, S. Yadir, S. Bounouar, C. Hajjaj, E. Baghaz, and M. El Aydi, "New method for extracting physical parameters of PV generators combining an implemented genetic algorithm and the simulated annealing algorithm," *Sol. Energy*, vol. 194, pp. 239–247, Dec. 2019.
[17] D. S. H. Chan and J. C. H. Phang, "Analytical methods for the extraction of solar-cell single- and double-diode model parameters from I–V characteristics," *IEEE Trans. Electron Devices*, vol. ED-34, no. 2, pp. 286–293, Feb. 1987.
[18] S. Gude and K. C. Jana, "Parameter extraction of photovoltaic cell using an improved cuckoo search optimization," *Sol. Energy*, vol. 204, pp. 280–293, Jul. 2020.
[19] V. Khanna, B. K. Das, D. Bisht, Vandana, and P. K. Singh, "A three diode model for industrial solar cells and estimation of solar cell parameters using PSO algorithm," *Renew. Energy*, vol. 78, pp. 105–113, Jun. 2015.
[20] J. Ma, Z. Bi, T. O. Ting, S. Hao, and W. Hao, "Comparative performance on photovoltaic model parameter identification via bio-inspired algorithms," *Sol. Energy*, vol. 132, pp. 606–616, Jul. 2016.
[21] R. A. P. Franco and F. H. T. Vieira, "Analytical method for extraction of the single-diode model parameters for photovoltaic panels from datasheet data," *Electron. Lett.*, vol. 54, no. 8, pp. 519–521, Apr. 2018.
[22] T. T. Yetayew and T. R. Jyothsna, "Parameter extraction of photovoltaic modules using Newton Raphson and simulated annealing techniques," in *Proc. IEEE Power, Commun. Inf. Technol. Conf. (PCITC)*, Oct. 2015, pp. 229–234.
[23] K. Et-Torabi, I. Nassar-eddine, A. Obbadi, Y. Errami, R. Rmaily, S. Sahnoun, A. El Fajri, and M. Agunaou, "Parameters estimation of the single and double diode photovoltaic models using a Gauss–Seidel algorithm and analytical method: A comparative study," *Energy Convers. Manage.*, vol. 148, pp. 1041–1054, Sep. 2017.
[24] H. Ibrahim and N. Anani, "Evaluation of analytical methods for parameter extraction of PV modules," *Energy Proc.*, vol. 134, pp. 69–78, Oct. 2017.
[25] I. Nassar-Eddine, A. Obbadi, Y. Errami, A. El Fajri, and M. Agunaou, "Parameter estimation of photovoltaic modules using iterative method and the Lambert W function: A comparative study," *Energy Convers. Manage.*, vol. 119, pp. 37–48, Jul. 2016.
[26] A. R. Jordehi, "Parameter estimation of solar photovoltaic (PV) cells: A review," *Renew. Sustain. Energy Rev.*, vol. 61, pp. 354–371, 2016.
[27] W. De Soto, S. A. Klein, and W. A. Beckman, "Improvement and validation of a model for photovoltaic array performance," *Sol. Energy*, vol. 80, no. 1, pp. 78–88, 2006.
[28] R. Gottschalg, M. Rommel, D. G. Infield, and M. Kearney, "The influence of the measurement environment on the accuracy of the extraction of the physical parameters of solar cells," *Meas. Sci. Technol.*, vol. 10, no. 9, p. 796, 1999.
[29] C. Li, Y. He, D. Xiao, Z. Luo, J. Fan, and P. X. Liu, "A novel hybrid approach of ABC with SCA for the parameter optimization of SVR in blind image quality assessment," *Neural Comput. Appl.*, vol. 34, pp. 1–27, Jan. 2022.
[30] M. Li, C. Li, Z. Huang, J. Huang, G. Wang, and P. X. Liu, "Spiral-based chaotic chicken swarm optimization algorithm for parameters identification of photovoltaic models," *Soft Comput.*, vol. 25, no. 20, pp. 12875–12898, Oct. 2021.
[31] Z. Yan, L. Chunquan, S. Zhenshou, L. Xiong, and A. C. Luo, "An improved brain storming optimization algorithm for estimating parameters of photovoltaic models," *IEEE Access*, vol. 7, pp. 77629–77641, 2019.
[32] M. Khajehzadeh, M. R. Taha, A. El-Shafie, and M. Eslami, "Search for critical failure surface in slope stability analysis by gravitational search algorithm," *Int. J. Phys. Sci.*, vol. 6, no. 21, pp. 5012–5021, 2011.
[33] M. Eslami, H. Shareef, and A. Mohamed, "Optimization and coordination of damping controls for optimal oscillations damping in multi-machine power system," *Int. Rev. Electr. Eng.*, vol. 6, no. 4, pp. 1984–1993, 2011.
[34] V. J. Chin, Z. Salam, and K. Ishaque, "Cell modelling and model parameters estimation techniques for photovoltaic simulator application: A review," *Appl. Energy*, vol. 154, pp. 500–519, Sep. 2015.
[35] M. Zagrouba, A. Sellami, M. Bouaïcha, and M. Ksouri, "Identification of PV solar cells and modules parameters using the genetic algorithms: Application to maximum power extraction," *Solar Energy*, vol. 84, no. 5, pp. 860–866, 2010.
[36] J. Liang, S. Ge, B. Qu, K. Yu, F. Liu, H. Yang, P. Wei, and Z. Li, "Classified perturbation mutation based particle swarm optimization algorithm for parameters extraction of photovoltaic models," *Energy Convers. Manage.*, vol. 203, Jan. 2020, Art. no. 112138.

[37] M. Eslami, H. Shareef, A. Mohamed, and M. Khajehzadeh, "Optimal location of PSS using improved PSO with chaotic sequence," in *Proc. Int. Conf. Electr., Control Comput. Eng. (InECCE)*, Jun. 2011, pp. 253–258.
[38] K. M. El-Naggar, M. R. AlRashidi, M. F. AlHajri, and A. K. Al-Othman, "Simulated annealing algorithm for photovoltaic parameters identification," *Sol. Energy*, vol. 86, no. 1, pp. 266–274, Jan. 2012.
[39] A. Askarzadeh and A. Rezazadeh, "Parameter identification for solar cell models using harmony search-based algorithms," *Sol. Energy*, vol. 86, no. 11, pp. 3241–3249, Nov. 2012.
[40] N. Rajasekar, N. K. Kumar, and R. Venugopalan, "Bacterial foraging algorithm based solar PV parameter estimation," *Sol. Energy*, vol. 97, pp. 255–265, Nov. 2013.
[41] M. A. Awadallah, "Variations of the bacterial foraging algorithm for the extraction of PV module parameters from nameplate data," *Energy Convers. Manage.*, vol. 113, pp. 312–320, Apr. 2016.
[42] S. Li, W. Gong, X. Yan, C. Hu, D. Bai, L. Wang, and L. Gao, "Parameter extraction of photovoltaic models using an improved teaching-learning-based optimization," *Energy Convers. Manage.*, vol. 186, pp. 293–305, Apr. 2019.
[43] W. Long, S. Cai, J. Jiao, M. Xu, and T. Wu, "A new hybrid algorithm based on grey wolf optimizer and cuckoo search for parameter extraction of solar photovoltaic models," *Energy Convers. Manage.*, vol. 203, Jan. 2020, Art. no. 112243.
[44] L. Guo, Z. Meng, Y. Sun, and L. Wang, "Parameter identification and sensitivity analysis of solar cell models with cat swarm optimization algorithm," *Energy Convers. Manage.*, vol. 108, pp. 520–528, Jan. 2016.
[45] S. Li, Q. Gu, W. Gong, and B. Ning, "An enhanced adaptive differential evolution algorithm for parameter extraction of photovoltaic models," *Energy Convers. Manage.*, vol. 205, Feb. 2020, Art. no. 112443.
[46] G. Xiong, J. Zhang, D. Shi, and Y. He, "Parameter extraction of solar photovoltaic models using an improved whale optimization algorithm," *Energy Convers. Manage.*, vol. 174, pp. 388–405, Oct. 2018.
[47] Y. Zhang, M. Ma, and Z. Jin, "Comprehensive learning Jaya algorithm for parameter extraction of photovoltaic models," *Energy*, vol. 211, Nov. 2020, Art. no. 118644.
[48] A. M. Beigi and A. Maroosi, "Parameter identification for solar cells and module using a hybrid firefly and pattern search algorithms," *Sol. Energy*, vol. 171, no. 1, pp. 435–446, Sep. 2018.
[49] M. Khajehzadeh, M. R. Taha, and M. Eslami, "A new hybrid firefly algorithm for foundation optimization," *Nat. Acad. Sci. Lett.*, vol. 36, no. 3, pp. 279–288, Jun. 2013.
[50] D. Oliva, E. Cuevas, and G. Pajares, "Parameter identification of solar cells using artificial bee colony optimization," *Energy*, vol. 72, pp. 93–102, Aug. 2014.
[51] R. Sarjila, K. Ravi, J. B. Edward, K. S. Kumar, and A. Prasad, "Parameter extraction of solar photovoltaic modules using gravitational search algorithm," *J. Electr. Comput. Eng.*, vol. 2016, pp. 1–6, Dec. 2016.
[52] M. Khajehzadeh, M. R. Taha, and M. Eslami, "Multi-objective optimization of foundation using global-local gravitational search algorithm," *Struct. Eng. Mech.*, vol. 50, no. 3, pp. 257–273, May 2014.
[53] D. Allam, D. A. Yousri, and M. B. Eteiba, "Parameters extraction of the three diode model for the multi-crystalline solar cell/module using moth-flame optimization algorithm," *Energy Convers. Manage.*, vol. 123, pp. 535–548, Sep. 2016.
[54] C. Li, Z. Niu, Z. Song, B. Li, J. Fan, and P. X. Liu, "A double evolutionary learning moth-flame optimization for real-parameter global optimization problems," *IEEE Access*, vol. 6, pp. 76700–76727, 2018.
[55] Z. Huang, L. Chen, M. Li, P. X. Liu, and C. Li, "A multiple learning moth flame optimization algorithm with probability-based chaotic strategy for the parameters estimation of photovoltaic models," *J. Renew. Sustain. Energy*, vol. 13, no. 4, Jul. 2021, Art. no. 043502.
[56] J. Gupta, P. Nijhawan, and S. Ganguli, "Parameter extraction of solar PV cell models using novel metaheuristic chaotic tunicate swarm algorithm," *Int. Trans. Electr. Energy Syst.*, vol. 31, no. 12, p. e13244, Dec. 2021.
[57] A. T. Kiani, M. F. Nadeem, A. Ahmed, I. A. Sajjad, A. Raza, and I. A. Khan, "Chaotic inertia weight particle swarm optimization (CIW-PSO): An efficient technique for solar cell parameter estimation," in *Proc. 3rd Int. Conf. Comput., Math. Eng. Technol. (iCoMET)*, Jan. 2020, pp. 1–6.
[58] A. Ramadan, S. Kamel, M. H. Hassan, E. M. Ahmed, and H. M. Hasanien, "Accurate photovoltaic models based on an adaptive opposition artificial hummingbird algorithm," *Electronics*, vol. 11, no. 3, p. 318, Jan. 2022.
[59] D. F. Alam, D. A. Yousri, and M. B. Eteiba, "Flower pollination algorithm based solar PV parameter estimation," *Energy Convers. Manage.*, vol. 101, no. 1, pp. 410–422, Sep. 2015.
[60] M.-U.-N. Khursheed, M. A. Alghamdi, M. F. N. Khan, A. K. Khan, I. Khan, A. Ahmed, A. T. Kiani, and M. A. Khan, "PV model parameter estimation using modified FPA with dynamic switch probability and step size function," *IEEE Access*, vol. 9, pp. 42027–42044, 2021.
[61] S. Kaur, L. K. Awasthi, A. L. Sangal, and G. Dhiman, "Tunicate swarm algorithm: A new bio-inspired based metaheuristic paradigm for global optimization," *Eng. Appl. Artif. Intell.*, vol. 90, Apr. 2020, Art. no. 103541.
[62] J. Wang, S. Wang, and Z. Li, "Wind speed deterministic forecasting and probabilistic interval forecasting approach based on deep learning, modified tunicate swarm algorithm, and quantile regression," *Renew. Energy*, vol. 179, pp. 1246–1261, Dec. 2021.
[63] D. H. Wolper and W. G. Macready, "No free lunch theorems for optimization," *IEEE Trans. Evol. Comput.*, vol. 1, no. 1, pp. 67–82, Apr. 1997.
[64] M. R. AlRashidi, M. F. AlHajri, K. M. El-Naggar, and A. K. Al-Othman, "A new estimation approach for determining the I–V characteristics of solar cells," *Sol. Energy*, vol. 85, no. 7, pp. 1543–1550, Jul. 2011.
[65] H. Tian, F. Mancilla-David, K. Ellis, E. Muljadi, and P. Jenkins, "A cell-to-module-to-array detailed model for photovoltaic panels," *Sol. Energy*, vol. 86, no. 9, pp. 2695–2706, Sep. 2012.
[66] T. Easwarakhanthan, J. Bottin, I. Bouhouch, and C. Boutrit, "Nonlinear minimization algorithm for determining the solar cell parameters with microcomputers," *Int. J. Sol. Energy*, vol. 4, no. 1, pp. 1–12, 1986.
[67] Q. Niu, H. Zhang, and K. Li, "An improved TLBO with elite strategy for parameters identification of PEM fuel cell and solar cell models," *Int. J. Hydrogen Energy*, vol. 39, no. 8, pp. 3837–3854, 2018.
[68] X. Chen, K. Yu, W. Du, W. Zhao, and G. Liu, "Parameters identification of solar cell models using generalized oppositional teaching learning based optimization," *Energy*, vol. 99, pp. 170–180, Mar. 2016.
[69] Z. Wu, D. Yu, and X. Kang, "Parameter identification of photovoltaic cell model based on improved ant lion optimizer," *Energy Convers. Manage.*, vol. 151, pp. 107–115, Nov. 2017.
[70] K. Yu, J. J. Liang, B. Y. Qu, X. Chen, and H. Wang, "Parameters identification of photovoltaic models using an improved JAYA optimization algorithm," *Energy Convers. Manage.*, vol. 150, pp. 742–753, Oct. 2017.
[71] S. J. Patel, A. K. Panchal, and V. Kheraj, "Extraction of solar cell parameters from a single current–voltage characteristic using teaching learning based optimization algorithm," *Appl. Energy*, vol. 119, pp. 384–393, Apr. 2014.

BEHDAD ARANDIAN received the Ph.D. degree in electrical engineering from the Amirkabir University of Technology, Tehran, Iran, in 2017. He is currently an Associate Professor with the Electrical Engineering Department, Islamic Azad University, Isfahan, Iran. His current research interests include the energy planning (renewable and non-renewable resources), optimization methods, and power system planning.

MAHDIYEH ESLAMI (Member, IEEE) received the B.Sc. degree in electrical engineering from the Shahid Bahonar University of Kerman, Iran, in 2000, the M.Sc. degree in electrical engineering from the Iran University of Science and Technology (IUST), Tehran, Iran, in 2004, and the Ph.D. degree in electrical engineering from the National University of Malaysia (UKM), in 2012. From 2012 to 2013, she was a Postdoctoral Research Fellow with the Power Research Group, UKM. She is currently an Assistant Professor with the Department of Electrical Engineering, Islamic Azad University, Kerman. Since her Ph.D. degree, she has been publishing more than 80 articles in various fields related to power system. Her research interests include power system stability, application of AI techniques in power systems, power system dynamics, and FACTS devices.

SAIFULNIZAM ABD. KHALID received the B.Eng., M.E.E., and Ph.D. degrees from Universiti Teknologi Malaysia, Johor Bahru, Malaysia, in 1998, 2000, and 2009, respectively. He is currently an Associate Professor at the School of Electrical Engineering, Faculty of Engineering, Universiti Teknologi Malaysia. His research interests include deregulated power systems, application of artificial neural network in power systems, power tracing, and smart metering applications.

BASEEM KHAN (Senior Member, IEEE) received the B.Eng. degree in electrical engineering from Rajiv Gandhi Technological University, Bhopal, India, in 2008, and the M.Tech. and D.Phil. degrees in electrical engineering from the Maulana Azad National Institute of Technology, Bhopal, in 2010 and 2014, respectively. He is currently working as a Faculty Member at Hawassa University, Ethiopia. He has published more than 100 research papers in well reputable research journals, including IEEE TRANSACTION, IEEE ACCESS, *Computers and Electrical Engineering* (Elsevier), *IET GTD*, *IET RPG*, and *IET Power Electronics*. Further, he has published, authored, and edited books with Wiley, CRC Press, and Elsevier. His research interests include power system restructuring, power system planning, smart grid technologies, meta-heuristic optimization techniques, reliability analysis of renewable energy systems, power quality analysis, and renewable energy integration.

USMAN ULLAH SHEIKH (Senior Member, IEEE) received the Ph.D. degree in image processing and computer vision from Universiti Teknologi Malaysia, in 2009. He is currently a Senior Lecturer with the Department of Computer and Electrical Engineering, Faculty of Engineering, Universiti Teknologi Malaysia. His research interests include computer vision, machine learning, and embedded systems design.

EHSAN AKBARI was born in Borujerd, Iran, in 1987. He received the B.Sc. and M.Sc. degrees in power electrical engineering from the Mazandaran University of Science and Technology (MUST), Babol, Iran, in 2010 and 2014, respectively. He has published more than 125 papers in reputed journals and conferences. His research interests include power quality and distribution flexible AC transmission systems (DFACTS), application of power electronics in power systems, power electronics multilevel converters, smart grids, harmonics and reactive power control using hybrid filters, and renewable energy systems. He is a Contributing Reviewer of *AJEEE* journal.

ADIL HUSSEIN MOHAMMED received the B.Sc. degree in electrical and electronic engineering and the M.Sc. degree in communication engineering. He is currently an Assistant Lecturer (Full) at the Department of Communication and Computer, Cihan University-Erbil, Kurdistan Region, Iraq.